

WEATHERING OF SPODUMENE TO SMECTITE IN A LATERITIC ENVIRONMENT

BALBIR SINGH* AND R. J. GILKES

Soil Science and Plant Nutrition, School of Agriculture
The University of Western Australia, Nedlands WA 6009 Australia

Abstract—Weathering of spodumene in a lateritized pegmatite in Western Australia was studied by investigating *in situ* samples by electron-beam techniques. The spodumene had mostly altered to smectite. However, some non-crystalline material adjacent to smectite and intermixed with smectite was also observed. No crystallographic orientation between spodumene and smectite was observed by high resolution techniques. The spodumene dissolved to produce etch pits similar to those observed on hornblende grains. The etch pits were almost completely filled with smectite. Most of the Li in the spodumene was lost during its weathering to smectite.

Key Words—Ion-beam thinning, Non-crystalline weathering products, Smectite, Spodumene, Transmission electron microscopy.

INTRODUCTION

The alteration of pyriboles to clay minerals has been studied by several workers who have identified crystallographic relations between the parent chain structure and the layer structure of secondary clay minerals. Conversion of amphiboles to micas occurs in metamorphic reactions (Veblen and Buseck, 1980), and replacement of pyroxene by pseudomorphs of vermiculite may occur with a high degree of preferred orientation (Basham, 1974). Wilson (1975) predicted that pyroxenes such as enstatite can transform to a layer structure with minimum reorganization, if the *cb* plane of the enstatite becomes the *ab* plane of layer silicate by coalescence of chains to form a tetrahedral sheet. This type of topotactic transformation has been observed by high resolution transmission electron microscopy (HRTEM) for hedenbergite altering to nontronite (Eggleton, 1975) and enstatite altering to talc (Eggleton and Boland, 1982). However, not all pyriboles weather to clay minerals by topotactic transformation. A number of studies have shown that weathering of hornblende may proceed by congruent dissolution along crystallographic directions and precipitation of clay minerals and iron oxides from solution with no crystallographic relationship persisting between hornblende and clay minerals (Berner and Schott, 1982; Anand and Gilkes, 1984; Velbel, 1989; Argast, 1991). Topotaxial transformation of pyriboles to layer silicates is presumably facilitated if minimum adjustments in structure and composition are involved (Gilkes *et al.*, 1986). Thus pyriboles containing Mg, Fe, Al, and Si may readily alter to clay minerals and show topotactic relationship due to retention of these

ions as structural constituents in the clay minerals. In contrast, many pyriboles contain Ca or Na ions, which can only be retained in clay minerals as exchangeable cations. The behavior of Li in the pyroxene spodumene ($\text{LiAlSi}_2\text{O}_6$) during alteration to clay minerals cannot be so readily predicted as Li can occur in clay minerals both as an exchangeable cation and an octahedral cation (Brindley and Lemaitre, 1987). This paper examines the weathering of spodumene in a lateritic soil in southwestern Australia.

MATERIALS AND METHODS

Samples were taken from a deeply weathered spodumene bearing pegmatite in the Greenbushes Mineral Field, located in the southwest of western Australia approximately 300 km south of Perth (Williams, 1975). Intense chemical weathering has resulted in the development of an *in situ* lateritic profile over the mineralized pegmatite. A ferruginous duricrust and mottled zone are underlain by a pallid zone that extends to depths of up to 60 m. The samples were taken from the base of the open cut mine where the fabric of the parent rock was intact but weathering had begun (*i.e.*, saprolite). Initiation of weathering of spodumene can be recognized in the specimens by clouding of otherwise transparent grains.

A portion of the samples was impregnated with epoxy resin, and polished thin sections on glass slides were made for optical microscopy, electron microprobe analysis (EMPA), and scanning electron microscopy (SEM) using back-scattered electrons (BSE). Freshly exposed fracture surfaces of the samples were investigated by SEM using a Philips 505 instrument fitted with a BSE detector and energy dispersive X-ray analyzer (EDX). Specimens of about 1 cm³ volume were mounted on aluminum stubs, coated with carbon, and subsequently coated with a 5 nm thick layer of

* Present address: Department of Geology and Geophysics, University of California, Berkeley, California 94720-4767.

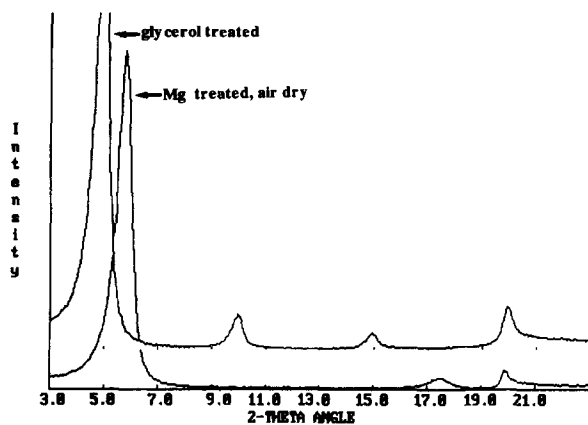


Figure 1. X-ray diffraction patterns of the basally oriented samples of the clay fraction separated from the partially weathered spodumene grains. The Mg-treated sample gave a reflection at about 15 Å, which expanded to 18 Å on glycerol treatment.

gold in a vacuum evaporator. Some partially weathered grains were ultrasonified in water to remove clay deposited in etch pits before SEM analysis. Samples for transmission electron microscopy (TEM) were prepared by two methods. A dilute suspension of a crushed sample was prepared in distilled water. The <10 µm fraction was separated from the bulk suspension and drops were placed on holey carbon films with a micropipette. The drops were dried under cover at room temperature. Partially weathered regions in the petrographic thin sections were removed and ion milled with Ar at 5 kV to prepare ultrathin sections for TEM investigation. The selected regions in the thin sections were examined by optical microscopy and SEM using BSE and EDX prior to removal from thin sections. All samples for TEM were investigated using a Philips EM 430 instrument operated at 300 kV.

Clay suspensions were deposited onto ceramic plates under suction to prepare oriented clay samples. The clay films were saturated with Mg, K, and glycerol for diagnostic purposes (Brown and Brindley, 1980). XRD patterns of the whole material and the clay films were obtained using Cu-K α radiation with a computer-controlled Philips vertical diffractometer and graphite diffracted beam monochromator. The digital XRD patterns were interpreted with the aid of XPAS analytical software (Singh and Gilkes, 1992). The elemental composition of spodumene and clay separated from partially weathered grains was determined by atomic absorption spectrophotometry of acid digests.

RESULTS AND DISCUSSION

Mineralogy and chemistry of bulk weathering products

XRD patterns of the <2 µm fraction of clay separated from partially weathered grains showed that smectite is the major crystalline weathering product

Table 1. The chemical composition of spodumene and Na-saturated smectite.

Oxide weight (%)	Spodumene	Smectite	% Loss/gain
SiO ₂	65.36	65.14	6
Al ₂ O ₃	26.93	25.32	0
MnO	0.03	0.15	414
Fe ₂ O ₃	0.09	0.81	828
MgO	0.10	0.08	-23
Li ₂ O	6.86	0.23	-97
CaO	0.29	0.01	-95
K ₂ O	0.06	0.23	285
Na ₂ O	0.27	3.14	1140
H ₂ O	0.00	4.90	
Total	99.99	100.01	
Volume	100	120	20

The loss/gain of elements has been calculated assuming that all Al is retained.

(Figure 1). The chemical compositions of the smectite and spodumene are shown in Table 1 and have an almost identical ratio of Al₂O₃/SiO₂. Assuming that all Al is conserved, weathering of spodumene to smectite would result in a 20% increase in volume (Table 1). Most Li and Ca have been lost, and moderate amounts of K, Mn, and Fe have been imported into the weathered material.

Petrography and morphology of weathering grains

A polished section of a spodumene grain in relatively advanced stage of weathering is shown in Figure 2. The boundary of the original spodumene grain is indicated by a continuous open channel around the partially weathered grain. The channel may have been caused by shrinking of smectite in the channel due to drying of the sample during preparation of the thin section. Much of the grain has been replaced by smectite within which residual fragments of the spodumene crystal are preserved in their original orientation. Etch pits on the spodumene grain formed by weathering mostly exhibit a strong crystallographic influence with their long axis parallel to the cleavage plane. A few etch pits, however, do not follow the cleavage plane. Cleavages in part of the crystal have widened due to dissolution as may be seen by comparing the width of cleavage slits in the fresh spodumene and those in altered regions of the grain. The widened slits exhibit denticulated walls and are filled with smectite. Most of the space originally occupied by the spodumene grain is filled with smectite. This is broadly consistent with the calculated volume of the smectite formed per unit volume of spodumene (shown in Table 1), which indicates that the entire space should be occupied with smectite. The smectite and spodumene in many regions are in contact, suggesting that weathering of spodumene in these areas has occurred either by diffusive solid state transformation, which may be via an amorphous phase, or

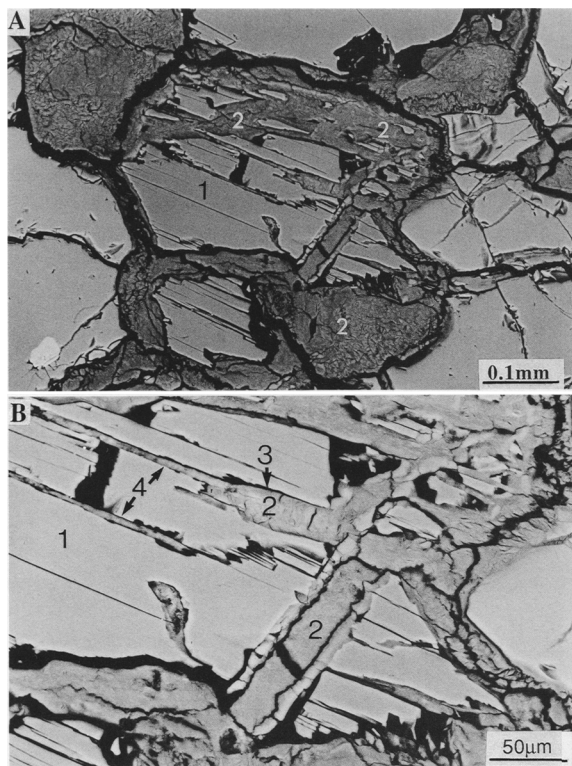


Figure 2. Back-scattered scanning electron micrographs of a polished section of partially weathered spodumene grain: A) Part of the spodumene (1) grain has been mostly replaced by smectite (2), and some residual fragments of the spodumene crystal, retaining their original orientation, are present within the smectite; B) an enlarged part of A, with smectite present in the dissolution etch pits (3) and cleavages (4).

by a process of dissolution and immediate precipitation of secondary products without much export of the released ions. Some small etch pits are devoid of weathering products, indicating that in these regions spodumene has dissolved and ions have migrated from the site, but presumably precipitation of smectite has occurred adjacent to the site of dissolution.

The surface morphology of partially weathered grains (Figure 3) that had been washed in water to expose etch pits shows features consistent with those observed in the polished thin sections. Extensive crystallographically controlled etch pits and sawtooth terminations are present. These features were probably mostly coated with clay, as some parts of the surface have remained coated with smectite. The shape and crystallographic orientation of saw-tooth terminations on spodumene are somewhat different from those that Velbel (1989) observed on hornblende grains. Saw-tooth terminations on hornblende were much sharper and had curved sides, with neither side being parallel to the z axis. Berner *et al.* (1980) suggested that saw-toothed terminations on hornblende are produced by coalescence of adjacent lenticular etch pits. Anand and Gilkes (1984)

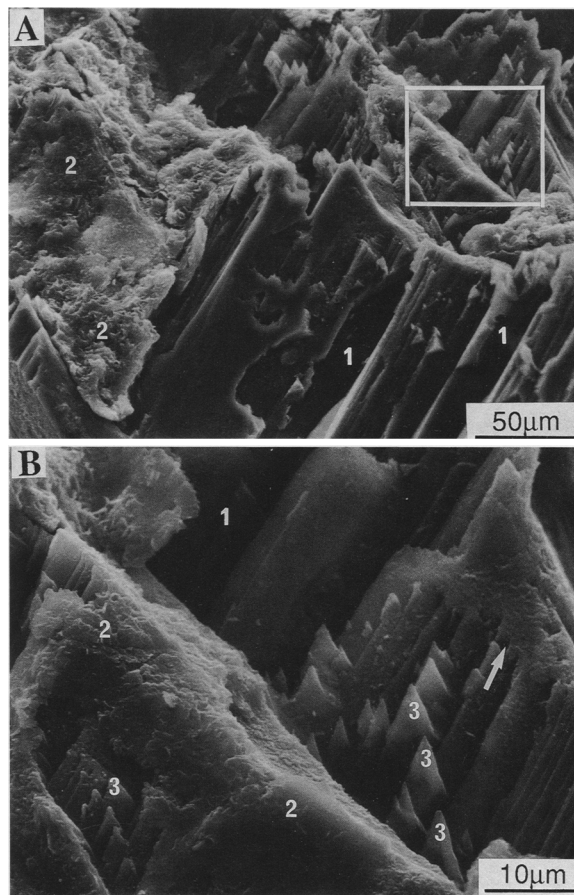


Figure 3. A) Scanning electron micrographs of a partially weathered spodumene grain. Etch pits (1) bounded by crystallographic planes and large masses of smectite (2) are present. B) An enlargement of the region marked in A. Saw tooth terminations (3) are present on the grain. Note that one side of the saw tooth appears to be parallel to the z crystallographic axis of spodumene (white arrow).

showed by electron diffraction that saw teeth were elongated along the z axis. Berner and Schott (1982), Velbel (1989), and Argast (1991) observed extensive lenticular etch pits on hornblende grains that were devoid of weathering products. Such lenticular etch pits are not present on spodumene grains. The terminations on spodumene have straight sides, one being parallel to the z axis. Apparently, the terminations on spodumene are not produced by coalescence of lenticular etch pits as described by Berner *et al.* (1980) for hornblende.

The surface of some of the unwashed spodumene grains contains circular dendritic growths of smectite (Figure 4), which appear to have developed from randomly distributed nuclei on the cleavage surfaces of spodumene grains. This essentially two-dimensional dendritic growth of smectite may be a consequence of crystal growth being confined within the planar cleavage voids within weathering spodumene crystals.

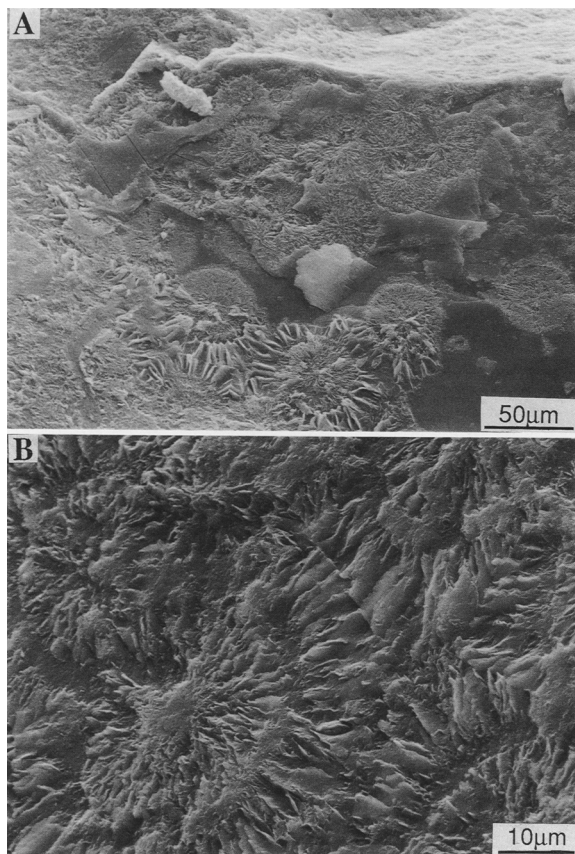


Figure 4. Scanning electron micrographs of the cleaved surfaces of a partially weathered spodumene grain: A) Circular dendritic aggregates of smectite extend over the spodumene surface; B) a magnified view of the dendritic smectite.

Weathering interface

The morphology of smectite described above is based on scanning electron microscopy. At this scale, it appears that smectite has crystallized from solution in voids, and subsequent shrinkage of the smectite (during specimen preparation?) has produced voids between the smectite and spodumene surfaces. In order to investigate the possibility of topotactic alteration of spodumene to smectite it is necessary to examine the undisturbed weathering interface using TEM. HRTEM of ultrathin sections of slightly to extensively weathered spodumene grains that show a range of features. In slightly weathered specimens, cleavages (Figure 5) contain layers of smectite that often appear to extend from cleavages into voids. The slit shaped cleavages containing smectite commonly exhibit irregular walls and are of variable width due to dissolution by circulating solutions. Some of the ions released by dissolution appear to have been carried out of the slits since the volume of smectite present does not account for the amount of spodumene dissolved. These ions may have contributed to the extensive growth of smec-

tite where slits open into large voids. Table 1 shows that alteration of spodumene to smectite results in a 20% increase in volume. Figure 5A shows crystalline packets of smectite crystals that have developed at the outlet of cleavage slits. The smectite layers appear to "feed" on the ions released by dissolution of spodumene within the slits. Some increase in the width of slits can also be caused by ion beam thinning if the slits are not completely impregnated by resin or if they have been eroded. The observed width in these samples is probably original since a similar increased width of slits was observed in the petrographic thin sections (Figure 1).

Smectite layers with their (001) face in contact with spodumene are present at many instances, but this may not represent the weathering interface. The actual weathering interface, where smectite layers are advancing and spodumene receding, may be found where the smectite crystals are growing toward the source of released ions. The source may be the adjacent spodumene surface or outlet of a channel carrying ions from cleavages in the spodumene crystal. In Figure 6, crystals of smectite appear to have grown into the spodumene crystal. This process may have resulted from enhanced dissolution of spodumene in front of growing smectite crystal. Presumably, flow of water towards and diffusion of ions from the weathering front is much more rapid parallel to plates of smectite crystals and within the interlamellar voids than perpendicular to the plates. Thus smectite crystals grow laterally into the spodumene. The smectite layers that have grown into spodumene are not parallel and do not appear to adopt directions reflecting the structure of the parent spodumene.

In more extensively weathered grains, a considerable amount of non-crystalline material, identified by electron diffraction, was present adjacent to the surface of the spodumene (Figure 7). The non-crystalline material exhibited a cell-like texture and did not contain voids. Large amounts of this amorphous material were also observed intermixed with smectite where spodumene had been completely replaced (Figure 8). The non-crystalline material, smectite, and spodumene had very similar $\text{Al}_2\text{O}_3/\text{Si}_2\text{O}_3$ ratios. The Li content of the non-crystalline material could not be determined, and it may be the critical factor in determining the crystallinity of the weathering products of spodumene.

DISCUSSION

Composition of smectite

Substitution of Li for Mg in trioctahedral smectite is common. Ianovici *et al.* (1990) reported Li-bearing smectites that contained 0.21 to 0.45 Li ions/unit cell as alteration products of magnesium silicate minerals. In this work, the dioctahedral smectite formed by weathering of spodumene contains only 0.12 Li ions/

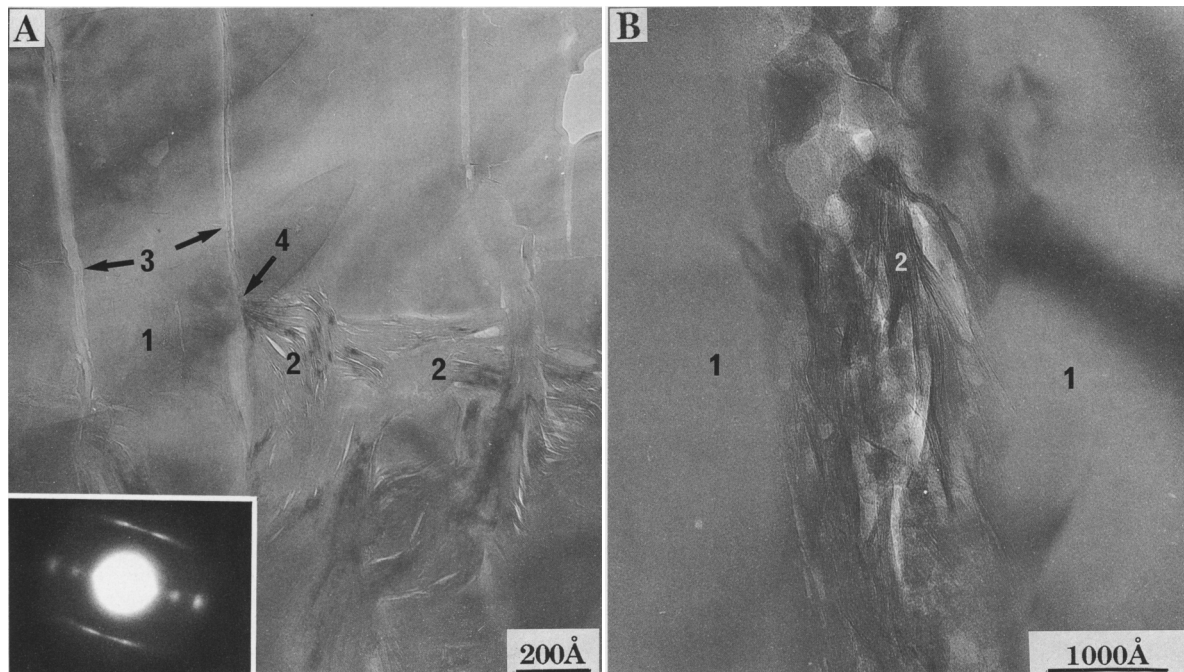


Figure 5. Transmission electron micrographs showing the alteration of spodumene (1) to smectite (2) in relation to cleavages (3). A) The cleavages have been widened by dissolution. Smectite appears to have crystallized within cleavages and where cleavages open into larger voids (4). The electron diffraction pattern of smectite shows basal reflections of ≈ 12 Å. B) Smectite layers occupy the entire volume of enlarged cleavages within a spodumene crystal.

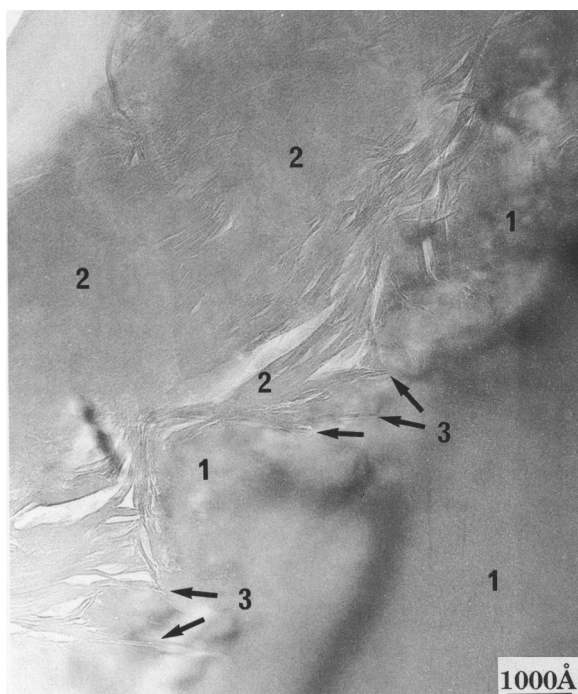


Figure 6. Transmission electron micrograph showing the direct alteration of spodumene (1) to smectite (2). At regions marked (3), the smectite crystals appear to have grown into the spodumene rather than simply coating the etched surface.

unit cell, which is much less than that for the smectites reported by Ianovici *et al.* (1990) and is only 3% of the original Li content of spodumene. No other crystalline alteration products that might retain Li were observed. Apparently, most of the Li was lost after breakdown of the spodumene structure. Topotactic alteration similar to that of hedenbergite to nontronite

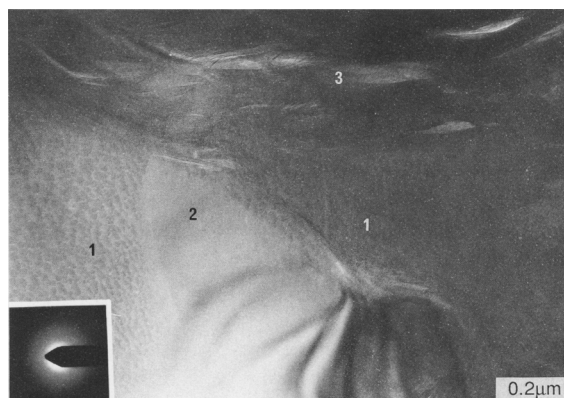


Figure 7. Transmission electron micrograph showing non-crystalline (1) material separating spodumene (2) and smectite (3). The non-crystalline material exhibits a nm-sized cell-like texture. Inset: a selected area diffraction pattern of the non-crystalline material showing characteristic diffuse rings.

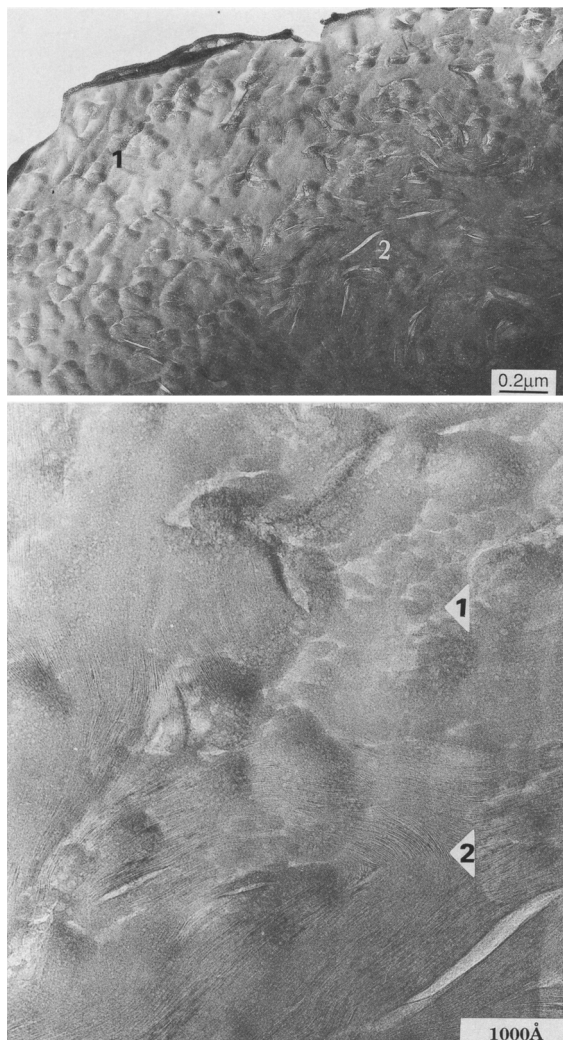


Figure 8. A) Transmission electron micrograph showing non-crystalline (1) material intermixed with smectite (2). The region containing smectite contains lenticular voids, whereas the non-crystalline material is massive. B) A magnified view of a region in Figure 7 showing interfingering of non-crystalline material (1) and smectite (2).

can conserve original cations (Eggleton, 1975), but no evidence for topotactic alteration of spodumene was obtained. Weathering of spodumene to smectite evidently proceeded via both solution and formation of a non-crystalline phase, and both processes involved the complete breakdown of the spodumene structure, thus exposing Li to losses by diffusion and leaching.

The $\text{Al}_2\text{O}_3/\text{Si}_2\text{O}_3$ ratios for spodumene and smectite are identical. Smectite has a relatively higher content of Fe, Mn and K. Apparently, these cations have been scavenged from solution and are ions released by weathering of other minerals. Except for the loss of most Li, the chemical composition of the smectite is similar to the composition of spodumene, which is

consistent with studies of weathering of feldspars and pyroxenes. This observation shows that the nature and chemical composition of the initial weathering product is commonly controlled by the composition of the parent mineral rather than by the macroscale environment, which may be influenced by the simultaneous weathering of other minerals in the rock (Eggleton and Qiming, 1991).

Amorphous weathering products

Non-crystalline products have been observed in studies of the weathering of K-feldspar and plagioclase. Eggleton and Buseck (1980) observed ring-shaped amorphous structures adjacent to weathering feldspar, that were considered to be an intermediary between feldspar and montmorillonite. Similarly, Banfield and Eggleton (1990) observed protocrystalline material as a compound intermediate between smectite and weathering plagioclase. In the present study the non-crystalline material appears to alter to smectite. In similar lateritic material from an adjacent locality, non-crystalline materials have not been observed where feldspar alters to kaolin (Anand and Gilkes, 1984). Non-crystalline material may occur in significant amounts only in poorly drained micro or macro environments, where it subsequently alters to smectite. In a relatively well-drained environment, smectite or kaolinite may form directly from solution or for some primary minerals via epitaxial alteration (e.g., biotite, Gilkes and Sudhiprakarn, 1979; muscovite, Singh and Gilkes, 1991).

CONCLUSIONS

In the pallid zone of a deeply weathered pegmatite, spodumene alters by a mechanism of dissolution and reprecipitation to a non-crystalline material and to smectite in relatively well-drained cracks and at grain surfaces. Most of the Li in spodumene was lost during alteration to smectite, although most Al and Si were conserved. The dissolution mechanism with etch pit formation in spodumene is similar to that for hornblende. No evidence was found of topotactic alteration of spodumene to smectite, which might be expected to occur considering the similarities of structure and chemical composition.

REFERENCES

- Anand, R. R. and Gilkes, R. J. (1984) Weathering of hornblende, plagioclase and chlorite in meta-dolerite, Australia: *Geoderma* **34**, 261–280.
- Argast, S. (1991) Chlorite vermiculitization and pyroxene etching in an aeolian periglacial sand dune, Allen county, Indiana: *Clays & Clay Minerals* **39**, 622–633.
- Banfield, J. F. and Eggleton, R. A. (1990) Analytical transmission electron microscope studies of plagioclase, muscovite, and K-feldspar weathering: *Clays & Clay Minerals* **38**, 77–89.
- Basham, I. R. (1974) Mineralogical changes associated with deep weathering of gabbro in Aberdeenshire: *Clay Miner.* **10**, 189–202.

- Berner, R. A. and Schott, J. (1982) Dissolution of pyroxenes and amphiboles during weathering: *Science* **207**, 1205–1206.
- Berner, R. A., Sjöberg, E. L., Velbel, M. A., and Krom, M. D. (1980) Mechanisms of pyroxene and amphibole weathering II Observation of soil grains: *Amer. J. Sci.* **282**, 1214–1231.
- Brindley, G. W. and Lemaître, J. (1987) Thermal, oxidation and reduction reactions of clay minerals: in *Chemistry of Clays and Clay Minerals*, A. C. D. Newman, ed., Mineralogical Society, London, 319–370.
- Brown, G. and Brindley, G. W. (1980) X-ray diffraction procedures for clay mineral identification: in *Crystal Structures of Clay Minerals and Their X-ray Identification*, G. W. Brindley and G. Brown, eds., Mineralogical Society, London, 305–309.
- Eggleton, R. A. (1975) Nontronite topotaxial after hedenbergite: *Amer. Mineral.* **60**, 1063–1068.
- Eggleton, R. A. and Boland, J. N. (1982) Weathering of enstatite to talc through a sequence of transitional phases: *Clays & Clay Minerals* **30**, 11–20.
- Eggleton, R. A. and Buseck, P. R. (1980) High resolution electron microscopy of feldspar weathering: *Clays & Clay Minerals* **28**, 173–178.
- Eggleton, R. A. and Qiming, W. (1991) Smectites formed by mineral weathering: *Proc. 7th Euroclay Conf., Dresden*, M. Storr, K.-H. Henning, and P. Adolphi, eds., Ernst-Moritz-Arndt Universität, Greifswald, 313–318.
- Gilkes, R. J. and Suddhiprakarn, A. (1979) Biotite alteration in deeply weathered granite. II The oriented growth of secondary minerals: *Clays & Clay Minerals* **37**, 361–367.
- Gilkes, R. J., Anand, R. R., and Suddhiprakarn, A. (1986) How the microfabric of soils may be influenced by the structure and chemical composition of parent minerals: *Trans. Int. Soil Sci. Conf. Hamburg* **6**, 1093–1106.
- Ianovici, V., Neacsu, G., and Neacsu, V. (1990) Li-bearing stevensite from Moldova Noua, Romania: *Clays & Clay Minerals* **38**, 171–178.
- Singh, Balbir and Gilkes, R. J. (1991) Weathering of chromian muscovite to kaolinite: *Clays & Clay Minerals* **39**, 571–579.
- Singh, Balbir and Gilkes, R. J. (1992) XPAS: An interactive computer program for analysis of powder X-ray diffraction patterns: *Powder Diffraction* **7**, 6–10.
- Veblen, D. R. and Buseck, P. R. (1980) Microstructures and reaction mechanisms in biopyriboles: *Amer. Mineral.* **65**, 599–623.
- Velbel, M. A. (1989) Weathering of hornblende to ferruginous products by a dissolution-precipitation mechanism: Petrography and stoichiometry: *Clays & Clay Minerals* **37**, 515–524.
- Williams, I. R. (1975) South Western province: in *Geology of Western Australia*, West. Australian Geol. Survey Mem. **2**, 65–69.
- Wilson, M. J. (1975) Chemical weathering of some primary rock-forming minerals: *Soil Sci.* **119**, 349–355.

(Received 12 November 1992; accepted 23 June 1993; Ms. 2297)